

The New Small-Drillhole Minipermeameter Probe for In-Situ Permeability Measurement (SPE 84595)



C.L. Dinwiddie (CNWRA, Southwest Research Institute*, 6220 Culebra Road, San Antonio, TX 78238-5166; e-mail: cdinwiddie@swri.org)

Abstract

Laboratory measurement of permeability using a Hassler cell is the industry standard; however, consistently removing undisturbed rock samples from friable outcrops is difficult. Although an alternative, the conventional surface-sealing minipermeameter, has been developed for permeability measurement, these devices suffer from difficulties in maintaining optimal forces on the tip seal when dealing with outcrop irregularities in the field; outcrop weathering is also problematic. Because a reliable field method is needed for outcrop studies, this paper presents an innovative technique for measuring permeability *in situ*. The design of a new small-drillhole minipermeameter probe is discussed, as well as the accompanying analytical technique and the size and shape of the instrument's averaging volume. Small diameter holes (1.8 cm) are drilled into an outcrop with a masonry drill, followed by drillhole vacuuming, probe insertion, seal expansion, gas injection, and calculation of the intrinsic permeability through measurement of the injection pressure, gas flow rate, and knowledge of the system geometry. Advantages of this approach are the elimination of questionable measurements from weathered outcrop surfaces, provision of a superior sealing mechanism around the air injection zone, and the potential for permeability measurement at multiple depths below an outcrop surface. To date, data have been collected from three diverse porous media: upper and lower shoreface sandstone (Escalante, Utah), saproclitic soils (Clemson, South Carolina), and nonwelded tuff (Bishop, California). The probe has proved durable and robust, with a single probe being sufficient to make thousands of measurements in a variety of environments. Data quality supports the conclusion that the drillhole probe is a practical field instrument.

Introduction

Meter-to-micrometer scale heterogeneities associated with beds, laminae, internal sedimentary structures and variations in pore morphology are the source of most retrieval difficulties during enhanced oil recovery.

Permeability Measurement - A Brief History

- **Traditional Method:** Measurement via core plug extraction at 30-cm intervals and using a Hassler sleeve or cell (one-dimensional gas flow); Data collection is at an ill-defined geologic scale, falling within the range of laminae and lamina sets
- **Contemporary Method:** Measurement at the scale of geologic heterogeneity with the conventional, surface-sealing minipermeameter (multi-dimensional gas flow); Data collection at much greater and statistically significant sampling densities

The Conventional, Surface-Sealing Minipermeameter (Figure 1)

- Release nitrogen gas into porous medium through a tip seal
- Measure steady state gas flow rate at associated injection pressure
- Use knowledge of the above variables and the system geometry in a form of Darcy's law to solve for permeability

Sources of Uncertainty When Used in the Field

- Accuracy is operator dependent; a consistent force must be used on the tip seal, thus this probe is prone to seal quality problems
- Field measurements are susceptible to natural weathering processes that alter the permeability of exposed outcrop surfaces

This Probe is Recommended for Laboratory Conditions Only

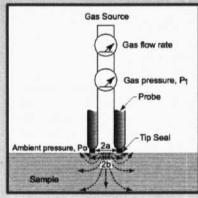


Figure 1. After Hurst et al. (1995)

- New method for outcrop studies: Multidimensional flow induced by a small-drillhole minipermeameter probe at some depth below the weathering rind (Molz et al., 2002)

Motivation

Permeability data were sought from the shallow-marine Upper Cretaceous Straight Cliffs formation (an analog to the heavy oil sands of the Temblor formation, Coalinga, California (Castle et al., 2000, 2003)) near Escalante, Utah. Being cognizant of the need to avoid measurements obtained from weathered surfaces, a core drill was selected to retrieve plugs from which permeability data could be collected in a laboratory environment on the distal and less weathered end. Because the sandstone outcrops were weakly cemented and friable the core drill frequently produced pulverized sand or significantly disturbed plugs. Thus, obtaining sandstone samples for use in the lab was generally not feasible at this site.

Drilling small, high quality holes in the sandstone outcrop, however, was found to be a simple task. The idea was conceived for a small minipermeameter field probe that would be inserted into a drilled hole, bypassing the weathered zone. Advantages of this *in situ* approach are:

- Minimization of the influence of weathering on permeability
- Provision of a superior sealing mechanism around the air injection zone (with which it is a simple matter to consistently apply the necessary force for a seal, while maintaining a geometrical factor that is independent of the operator)
- The potential for measurements at multiple depths below the outcrop surface

Small-Drillhole Minipermeameter System

- Operates by the same general principle as the conventional probe
- Suitable for field use because:
 - The sealing device is not operator dependent
 - Drilling small holes into an outcrop will bypass the most greatly weathered media

Methodology

Application of the small-drillhole minipermeameter probe is performed as follows: 1) the distal end of the probe is inserted into a previously drilled and vacuumed hole until the faceplate contacts the conical end of the drill hole; 2) the torque wheel is rotated clockwise, causing the seal to expand like a packer against the walls of the drillhole (Figure 2); 3) pressurized nitrogen gas is introduced into the porous medium through the injection zone; 4) once steady-state conditions have been achieved, pressure and flow rate are recorded, completing the test; finally, 5) the rotation of the torque wheel is reversed such that the compressive force on the rubber packer is reduced, breaking the seal and allowing it to return to its original unexpanded configuration. The probe is then removed from the drill hole for reuse.

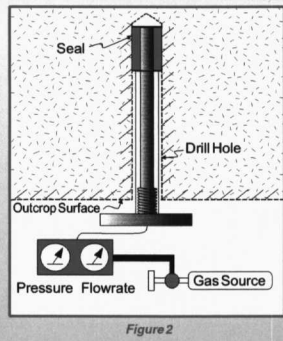


Figure 2

Methodology (Continued)

Probe Design

- The prototype was designed for use in a drillhole of 1.78-cm diameter, which was cut with a 1.55-cm masonry drillbit (Figure 3)
- The prototype was designed for use in a drillhole with a maximum depth of 10.2 cm; greater depths are possible with redesign
- Rotating the torque wheel clockwise on the threaded axial gas flow tube moves the sliding sleeve toward the distal end of the probe, causing the seal to axially compress and radially expand
- The seal is composed of smooth-finish pure gum rubber tubing
- A junction box is threaded onto the proximal end of the interior axial flow tube, providing a connection from the probe to an external gas source, and functioning as an endcap to the probe
- A static pressure capillary extends the distance from the junction box at the proximal end of the probe to the distal end, where the gas is delivered to the medium at some elevated injection pressure

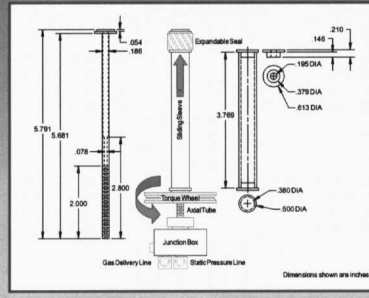


Figure 3

- Gas arrives at an adjustable L-fitting via flexible tubing from an external source, and flows within the junction box to the axial gas delivery tube

Instrumentation

- A commercially available minipermeameter data acquisition system (Figure 4) was adapted for use with the new drillhole probe (Chandler et al., 1988). The system interfaces with a portable PC through a software package that facilitates input of user-specified parameters (such as stabilization criteria and a geometrical factor that is appropriate for the drill hole and probe geometry) and that enables data acquisition, pressure transducer calibration, permeability computation, and data logging
- Retrofitting the flow and static pressure lines that link the new probe to the conventional minipermeameter instrumentation system was the only modification made to the 15-kg ABS plastic case containing:
 - Pressure transducer (absolute reference format with a full scale of 0.34 MPa, and an accuracy of ±0.1% of full scale)
 - Three flow meters (calibrated for measuring nitrogen flow rates of 0-30 cc/min, 0-600 cc/min, and 0-2000 cc/min at the standard reference pressure and temperature)
 - RTD probe
 - Data acquisition modules
 - Flow control valves and shut-off valve
 - 12-V lead-acid-gel battery



Figure 4

Analytical Technique

- Calculation of Apparent Permeability, k_g
- For minipermeameter flow, Darcy's law is:

$$k_g = \frac{\mu_g q_v P_i}{a G_o \left(\frac{P_i^2 - P_a^2}{2} \right)}$$

- μ_g = viscosity of N_2 gas at P_i and $T_{ambient}$, known
- q_v = volumetric flow rate, measured
- a = drillhole radius (0.89 cm)
- G_o = geometrical factor, from a numerical solution (949)
- P_i = injection pressure, measured
- P_a = atmospheric pressure, measured
- $T_{ambient}$ = ambient temperature, measured

- Geometrical Factor, G_o
- The geometrical factor, G_o , when calculated numerically for a given sample and probe geometry accounts for the complex multidimensional flow pattern throughout the porous medium, capturing the edge effects associated with the geometry of the drill hole and probe system (Figure 5). Geometrical factors were determined (Dinwiddie et al., 2003) for the small-drillhole minipermeameter probe as a function of varying flow system dimensions (i.e., drillhole depth, seal thickness, and injection area or vertical headspace), and are expressed in the form of geometrical factor curves (Figures 6-8).

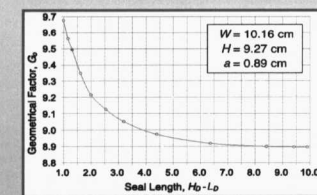


Figure 6

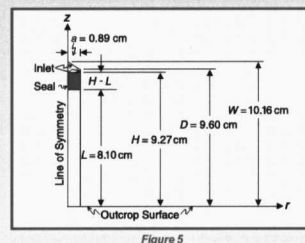


Figure 5

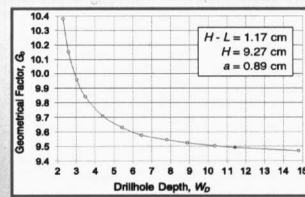


Figure 7

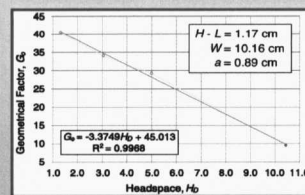


Figure 8

Methodology (Continued)

Averaging Volume

- Because the minipermeameter induces a diverging flow field, not all sub-volumes of the flow field contribute equally to the effective permeability value resulting from an integrated measurement by the instrument
- The size and shape of the instrumental window for the small-drillhole minipermeameter probe was determined (Dinwiddie, 2001; Molz et al., 2003) through an analysis of the unique instrument spatial weighting function, β_0 , which is physically given by the ratio of the steady-state energy dissipation rate at a given location per unit volume of medium, to the total energy dissipation rate over the entire flow domain

- When placed in dimensionless terms using $\phi_0 = (\phi - \phi_a)/(\phi_i - \phi_a)$, which is the formalism used by Goggin et al. (1986) for the dimensionless pseudopotential, ϕ_0 , one arrives at the simple and elegant dimensionless instrument spatial weighting function, $\beta_0(r_0, z_0)$, for the entire flow domain:

$$\beta_0(r_0, z_0) = \frac{|\nabla \phi_0|^2}{-G_o}$$

- Zones within the flow domain that are critical to the permeability measurement are identified clearly by elevated values of the spatial weighting function
- Porous medium volumes in the inlet vicinity are heavily weighted, with sub-volumes near the seal boundaries shown to be extremely important

- The integral of $\beta_0(r_0, z_0)$ over the entire flow domain is unity. By numerically integrating $\beta_0(r_0, z_0)$ over smaller volumes near the injection surface, the size and shape of the instrument averaging volume becomes apparent. Cylinders of influence were determined by integrating $\beta_0(r_0, z_0)$ over cylindrical sub-volumes in the near-neighborhood of the drillhole. From smallest to largest, the cylinders of influence illustrated in Figure 9 account for 2%, 23%, 74%, 94%, 97%, and 99% of the total weighting associated with the small-drillhole minipermeameter probe in a field configuration; over 90% of the volume "sensed" by the instrument is included within four drillhole radii of the drillhole apex

- The square of the pseudopotential gradient for several other representative geometries of the small-drillhole minipermeameter probe and sample domain are illustrated in Figure 10: (a) probe in a shallow drillhole; (b) probe with a thick seal; (c) probe that has not been fully inserted into the drilled hole. The contours illustrate the complex three-dimensional size and shape of the measurement averaging volume, while streamlines illustrate the flow geometry

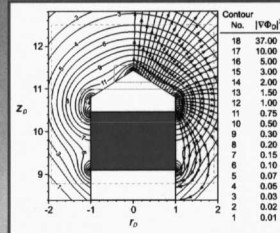


Figure 9

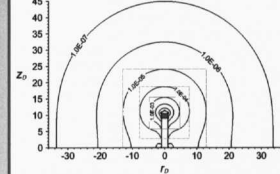


Figure 10(a)

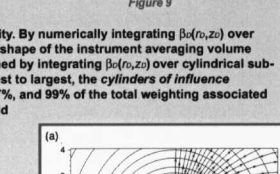


Figure 10(b)

Inaugural Field Study

Location and Stratigraphic Context

- The field site, an analog to the Temblor formation, Coalinga, California, is located approximately 13.7 km north and west of Escalante, Utah, within the Wide Ho'ow Reservoir Quadrangle (Figure 11); it is stratigraphically positioned within the shallow-marine John Henry member of the Upper Cretaceous Straight Cliffs formation, northeastern margin of the Kaiparowits Plateau, Utah

- Environments of deposition include coastal plain, estuarine, shoreface, and off-shore, which are analogous to those of the Temblor formation
- The Escalante location offers continuous exposures, minimally weathered outcrops, and well-defined stratigraphy

- The study site consists of lower shoreface and upper shoreface sandstone in intervals (Figure 12); the lower shoreface interval is composed of a bioturbated facies, while the upper shoreface interval is composed of a trough cross-bedded facies; the contact between the two intervals is laterally extensive, sharp, and locally y-zoned

- Permeability variations and lithologic characteristics that primary pores are larger and better-connected in the cross-bedded facies than in the bioturbated facies; special locations with the highest permeability values exhibit the largest amount of porosity and the least amount of clay and cement

- Permeability variations and lithologic characteristics that primary pores are larger and better-connected in the cross-bedded facies than in the bioturbated facies; special locations with the highest permeability values exhibit the largest amount of porosity and the least amount of clay and cement

- Permeability data, in combination with petrographic analyses, demonstrate facies-dependent variations in permeability caused by lithologic differences related to depositional processes at the Escalante, Utah site

Inaugural Field Study (Continued)

Data Collection

- Horizontal transects TD and TH are located in the lower shoreface bioturbated facies, while horizontal transect TX is located in the upper shoreface trough cross-bedded facies (Figures 13 and 14)
- Four vertical profiles (i.e., V1, V2, V3, V4) intersect the faces contact; a data profile was collected on each side of two ladders secured to the outcrop surface (Figures 13 and 14)
- Gas permeability data were collected in triplicate at approximately 510 locations on the sub-vertical face of the 6 x 21-m outcrop

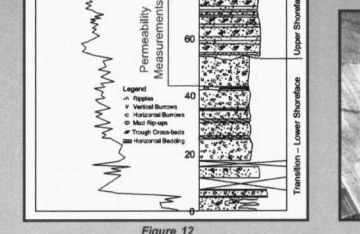


Figure 12

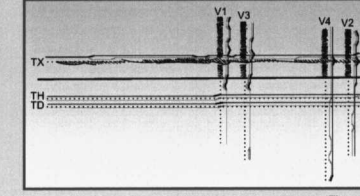


Figure 13

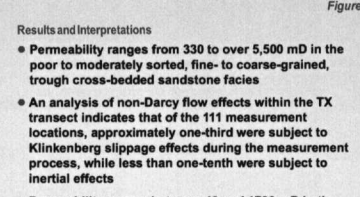


Figure 14

- Permeability ranges from 330 to over 5,500 mD in the poor to moderately sorted, fine- to coarse-grained, trough cross-bedded sandstone facies
- An analysis of non-Darcy flow effects within the TX transect indicates that of the 111 measurement locations, approximately one-third were subject to Klinkenberg slippage effects during the measurement process, while less than one-tenth were subject to inertial effects
- Permeability ranges between 40 and 1700 mD in the moderately to well-sorted, very fine- to fine-grained, massive-bedded bioturbated sandstone facies; within transect TD, in particular, there is little variability over a scale of several meters (Figure 15c)

- The low degree of variation in permeability within the bioturbated facies is interpreted as arising from homogenization by means of bioturbation, whereas the higher degree of permeability variation in the cross-bedded facies is attributed to primary heterogeneities associated with coarser grain size, greater primary porosity, and smaller percentages of clay matrix and cement
- Sedimentary structures in the cross-bedded facies included cross-bed foresets, and preferential flow pathways are also visible due to the presence of post-depositional iron staining

- Qualitative petrographic analyses indicate that primary pores are larger and better-connected in the cross-bedded facies than in the bioturbated facies; special locations with the highest permeability values exhibit the largest amount of porosity and the least amount of clay and cement
- Permeability variations and lithologic characteristics that primary pores are larger and better-connected in the cross-bedded facies than in the bioturbated facies; special locations with the highest permeability values exhibit the largest amount of porosity and the least amount of clay and cement

- Permeability data, in combination with petrographic analyses, demonstrate facies-dependent variations in permeability caused by lithologic differences related to depositional processes at the Escalante, Utah site

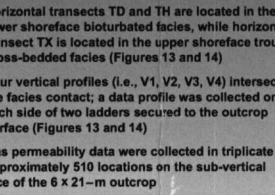


Figure 16

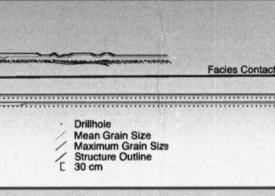


Figure 17

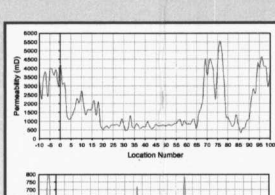


Figure 18

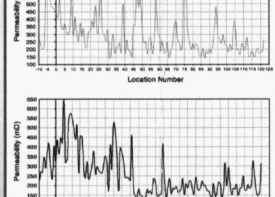


Figure 19

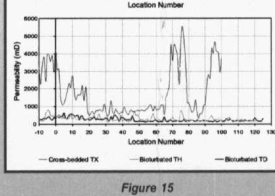


Figure 20

Inaugural Field Study (Continued)

Results and Interpretations (Continued)

- Horizontal transects TD and TH are located in the lower shoreface bioturbated facies, while horizontal transect TX is located in the upper shoreface trough cross-bedded facies (Figures 13 and 14)
- Four vertical profiles (i.e., V1, V2, V3, V4) intersect the faces contact; a data profile was collected on each side of two ladders secured to the outcrop surface (Figures 13 and 14)
- Gas permeability data were collected in triplicate at approximately 510 locations on the sub-vertical face of the 6 x 21-m outcrop

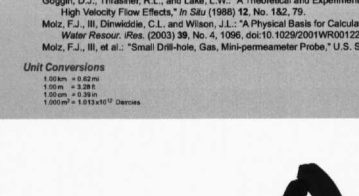
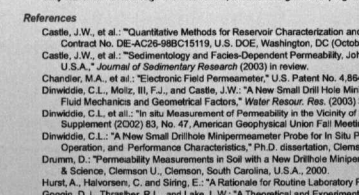
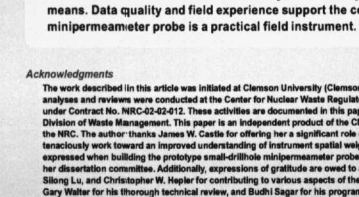
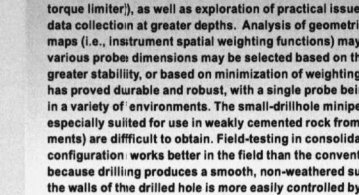
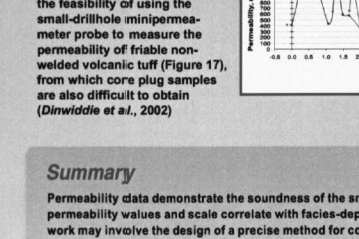
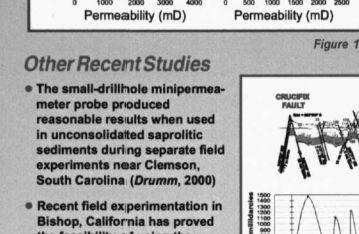


Figure 27

Other Recent Studies

- The small-drillhole minipermeameter probe produced reasonable results when used in unconsolidated saproclitic sediments during separate field experiments near Clemson, South Carolina (Drum, 2000)
- Recent field experimentation in Bishop, California has proved the feasibility of using the small-drillhole minipermeameter probe to measure the permeability of friable non-welded volcanic tuff (Figure 17), from which core plug samples are also difficult to obtain (Dinwiddie et al., 2002)

Summary

Permeability data demonstrate the soundness of the small-drillhole minipermeameter technique because permeability values and scale correlate with facies-dependent variations of geologic controls. Future work may involve the design of a precise method for consistently applying optimal seal pressures (e.g., a torque limiter), as well as exploration of practical issues involved in lengthening the drillhole probe for data collection at greater depths. Analysis of geometrical factor curves and measurement sensitivity maps (i.e., instrument spatial weighting functions) may suggest guidelines for future probe designs; e.g., various probe dimensions may be selected based on the regions of geometrical factor curves that exhibit greater stability, or based on minimization of weighting function singularities near the tip seal. The probe has proved durable and robust, with a single probe being sufficient to make thousands of measurements in a variety of environments. The small-drillhole minipermeameter probe has been shown to be especially suited for use in weakly cemented rock from which small core plugs (for laboratory measurements) are difficult to obtain. Field-testing in consolidated sandstone has indicated that this probe configuration works better in the field than the conventional surface-sealing minipermeameter probe because drilling produces a smooth, non-weathered surface and the normal force applied by the seal to the walls of the drilled hole is more easily controlled by a mechanical torque wheel than through human means. Data quality and field experience support the conclusion that the small-drillhole minipermeameter probe is a practical field instrument.

Acknowledgments

The work described in this article was initiated at Clemson University (Clemson, South Carolina) when the author was a Ph.D. candidate. Final data analyses and reviews were conducted at the Center for Nuclear Waste Regulatory Analyses (CNWRA) for the Nuclear Regulatory Commission (NRC) under Contract No. NRC-AC25-98BC15119, U.S. DOE, Washington, DC (October 2000). Castle, J.W., et al., "Sedimentology and Facies-Dependent Permeability, John Henry Member, Straight Cliffs Formation (Upper Cretaceous), Utah, U.S.A.," *Journal of Sedimentary Research* (2003) in review.

Chandler, M.A., et al., "Electronic Field Permeameter," U.S. Patent No. 4,864,845 (1989).

Dinwiddie, C.L., Molz, J.L., and Castle, J.W., "A New Small Drill Hole Minipermeameter Probe for In-Situ Permeability Measurement," *Fluid Mechanics and Geometrical Factors*, *Water Resour. Res.* (2003) 39, No. 7, 1178, doi:10.1029/2001WR001178.

Dinwiddie, C.L., et al., "In-Situ Measurement of Permeability in the Vicinity of Faulted Nonwelded Bioturbated Tuff," *Ess. Trans. AGU Fall Meeting Supplement* (2002) 83, No. 47, American Geophysical Union Fall Meeting, San Francisco, December 10.

Goggin, D.J., Thresher, R.L., and Lake, L.W., "A Theoretical and Experimental Analysis of Minipermeameter Response, Including Gas Slippage and High Velocity Flow Effects," *SPE* (1986) 12, No. 162, 79.

Molz, F.J., Dinwiddie, C.L., and Wilson, J.L., "A Physical Basis for Calculating Instrument Spatial Weighting Functions in Homogeneous Systems," *Water Resour. Res.* (2003) 39, No. 4, 1096, doi:10.1029/2001WR001220.

Molz, F.J., et al., "Small Drill-Hole, Gas Minipermeameter Probe," U.S. Statutory Invention Registration No. H2052 H (2002).

Unit Conversions
1 mD = 1 darcy
1 darcy = 9.863e-17 m²
1 cm = 0.03281 ft
1 ft = 0.3048 m

D-01